

Physics of grain boundaries in polycrystalline photovoltaic semiconductors

Yanfa Yan,^{1,a)} Wan-Jian Yin,¹ Yelong Wu,¹ Tingting Shi,¹ Naba R. Paudel,¹ Chen Li,² Jonathan Poplawsky,³ Zhiwei Wang,^{1,4} John Moseley,⁴ Harvey Guthrey,⁴ Helio Moutinho,⁴ Stephen J. Pennycook,⁵ and Mowafak M. Al-Jassim⁴

¹*Department of Physics and Astronomy and Wright Center for Photovoltaics Innovation and Commercialization, The University of Toledo, Ohio 43606, USA*

²*Materials Science and Technology Division, Oak Ridge National Laboratory, Oak Ridge, Tennessee 37831, USA*

³*The Center for Nanophase Materials Sciences, Oak Ridge National Laboratory, Oak Ridge, Tennessee 37831, USA*

⁴*National Renewable Energy Laboratory, Golden, Colorado 80401, USA*

⁵*Department of Materials Science and Engineering, University of Tennessee, Knoxville, Tennessee 37996, USA*

(Received 30 August 2014; accepted 9 October 2014; published online 16 March 2015)

Thin-film solar cells based on polycrystalline Cu(In,Ga)Se₂ (CIGS) and CdTe photovoltaic semiconductors have reached remarkable laboratory efficiencies. It is surprising that these thin-film polycrystalline solar cells can reach such high efficiencies despite containing a high density of grain boundaries (GBs), which would seem likely to be nonradiative recombination centers for photo-generated carriers. In this paper, we review our atomistic theoretical understanding of the physics of grain boundaries in CIGS and CdTe absorbers. We show that intrinsic GBs with dislocation cores exhibit deep gap states in both CIGS and CdTe. However, in each solar cell device, the GBs can be chemically modified to improve their photovoltaic properties. In CIGS cells, GBs are found to be Cu-rich and contain O impurities. Density-functional theory calculations reveal that such chemical changes within GBs can remove most of the unwanted gap states. In CdTe cells, GBs are found to contain a high concentration of Cl atoms. Cl atoms donate electrons, creating n-type GBs between p-type CdTe grains, forming local p-n-p junctions along GBs. This leads to enhanced current collections. Therefore, chemical modification of GBs allows for high efficiency polycrystalline CIGS and CdTe thin-film solar cells. © 2015 AIP Publishing LLC.

[<http://dx.doi.org/10.1063/1.4913833>]

I. INTRODUCTION

Cu(In, Ga)Se₂ (CIGS) and CdTe are promising absorber materials for thin-film photovoltaic applications. Both CIGS- and CdTe-based polycrystalline thin-film solar cell technologies have now achieved power conversion efficiencies at 21% for laboratory-scale cells.¹ Such high conversion efficiencies are truly remarkable because polycrystalline thin-film semiconductors are generally considered to exhibit poor optoelectronic properties compared to their single-crystal counterparts due to the existence of grain boundaries (GBs), which contain dislocation cores that typically create deep band gap levels and act as effective recombination centers, as the classic GB model concludes.^{2–4} Thus, GB passivation has been an important issue for polycrystalline thin-film solar cells.^{5,6}

There has been much debate regarding the roles of GBs in high efficiency CIGS and CdTe thin-film solar cells. While some experimental and theoretical results suggest that GBs could be beneficial to the cell performance, some others indicate the opposite effects of GBs, i.e., they are actually harmful to the cell performance. For example, Persson and Zunger^{7,8} proposed that GBs in CIGS could be neutral barriers to holes and therefore suppress carrier recombination,

which is beneficial to cell performance. The proposed neutral hole barriers have later been observed by scanning Kelvin probe microscopy and Hall measurements.^{9,10} The neutral GB model was based on the assumption that the polar (112) surfaces are stabilized by Cu vacancies.^{11–13} However, our high-resolution scanning transmission electron microscopy (STEM) images have shown clearly that grain boundaries with (112) planes in CIGS are not significantly Cu-poor.¹⁴ In fact, Abou-Ras and co-workers have observed by high-resolution STEM imaging, electron energy loss spectroscopy, and atom-probe tomography that some GBs in CIGS are Cu-rich.¹⁵ Therefore, the roles of GBs in CIGS are still under debate.^{16–23}

The roles of GBs in CdTe have also been unclear. It is well known that to produce high efficiencies CdTe-based thin-film solar cells must go through CdCl₂ heat treatment.^{24–27} Some results suggest that GBs could be beneficial for current collections. For example, Visoly-Fisher and co-workers have observed by conductive atomic force microscopy (C-AFM) measurement that GBs exhibit higher current than grain interiors.^{28,29} Our recent studies have shown that the higher currents at the vicinity of GBs are due to the segregation of Cl atoms during the CdCl₂ heat treatment.^{30,31} However, device simulations have indicated that GBs could be harmful to the open circuit voltage of the cells.^{32,33} Some studies have also shown that GBs in CdTe can be passivated

^{a)}Email: yanfa.yan@utoledo.edu

by Cl or Cu.^{34,35} Therefore, the CdCl₂ heat treatment can benefit the cell by GB, interface, and defect passivation.

In this paper, we review our atomistic theoretical understanding of the physics of GBs in CIGS and CdTe absorbers. As CIGS and CdTe are both based on the diamond structure, the GB structures should exhibit similar properties. We show that intrinsic GBs with dislocation cores in principle should create deep gap states and act as carrier recombination centers, which is harmful to device performance. However, in solar cell devices, the chemical changes at GBs can tune the GBs to be less harmful and even beneficial. For example, in CIGS cells, GBs could be Cu-rich and contain O impurities. Such chemical changes can remove most of the gap states. In CdTe cells, Cl atoms segregating into GBs can convert the GB regions to n-type, forming local p-n-p junctions, which improve current collections. Our results suggest that the properties of GBs can be tuned through chemical modifications, providing guidance for engineering polycrystalline thin-film solar cells to achieve improved performance.

II. COMPUTATION DETAILS

Our theoretical understanding of the physics of GBs in CIS and CdTe is based on the calculations of structural and electronic properties of GBs by density-functional theory (DFT) as implemented in the VASP code using the standard frozen-core projector augmented-wave (PAW) method.^{36–38} The cut-off energy for basis functions is 400 eV for CIS and 350 eV for CdTe. The general gradient approximation (GGA)+*U* method is used to open the band gap.^{39,40} Without *U*, the calculated band gap of CIS is zero. In our studies, we used *U* = 12 eV on the Cu 3*d* orbital, and the calculated band gap of CIS bulk as 0.68 eV. A *U* = 7 eV was used on the Cd 3*d* orbital and the calculated bulk band gap of CdTe was 0.98 eV. Both density of states (DOS) and band structures are used to understand the nature of gap states created by GBs. DOS plots and band structures provide complementary information. The combination of the two can provide more insight regarding the electronic information. Unlike previous studies using supercells containing two different but indispensable GBs with complementary orientation and polarities,^{14,18,34} we use supercells containing only single GBs to study the GB properties. The surface dangling bonds are passivated with pseudo-hydrogen to mimic the bulk properties.⁴¹ In this case, charge transfer between the two GBs in the previous model is no longer an issue.

III. RESULTS AND DISCUSSIONS

We first discuss the structures of CIS and CdTe. It is interesting to note that the two record holding solar cell absorbers, CdTe and CIS, have similar crystal structures, which can be described from the basic diamond structure. The dashed boxes indicate the unit cells. CdTe can be described by the stacking alternating Cd and Te layers. CIS can be described by alternately stacking a Se layer and a mixed Cu and In layer. Figures 1(a) and 1(b) show the structures of CdTe and CIS, respectively, projected approximately along the [110] direction. If atoms are only

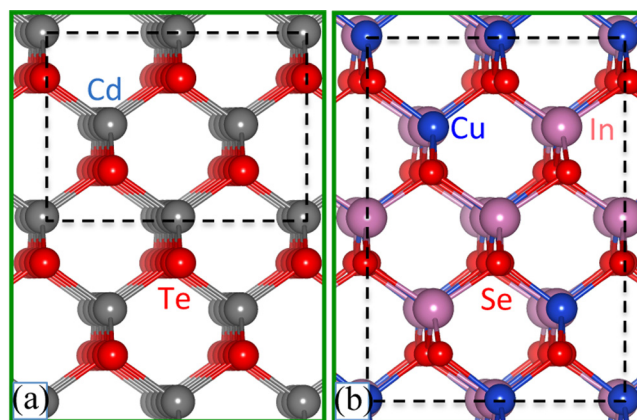


FIG. 1. Atomic structures of (a) CdTe and (b) CIS.

categorized by cation and anion atoms, CdTe and CIS would look the same. This structural similarity will allow us to acknowledge general conclusions regarding the physics of GBs in cation-anion compound semiconductors.

Due to their structural similarity, the structures of lattice defects, such as lamellar twins, stacking faults, and grain boundaries, can be expected to be similar in CIS and CdTe. Atomic-resolution STEM images of the same types of GBs obtained in CIS and CdTe are compared in Figs. 2(a) and 2(b), showing the atomic-resolution aberration-corrected STEM Z-contrast images of $\Sigma 3$ GBs. The GB planes are indicated by the white dashed lines. The GB plane is a (112) plane for the GB in CdTe, while it is a (114) plane in CIGS, due to multiple types of cation atoms in CIGS.⁴² As STEM Z-contrast images are sensitive to atomic number, we are able to distinguish cation and anion columns directly from their image intensities. As the column intensity at GB cores could be affected by strain, impurities or vacancies, we identify the cation-anion polarity at the cores by extrapolating from the surrounding perfect crystal.^{43,44}

As CdTe and CIS are compound semiconductors, GBs in CdTe and CIGS can be either cation-rich (with more cation atoms having unsaturated bonds) or anion-rich (with more anion atoms having unsaturated bonds). Figures 3(a) and 3(b) show the atomic structures of anion-terminated $\Sigma 3$ GBs in CdTe and CIGS, respectively. The atoms are color coded and marked in Fig. 3. These GBs contain dislocation cores, which are expected to exhibit dangling bonds, extra bonds, and wrong bonds. The atoms marked by Te1, Te2, Se1, and Se2 have unsaturated (dangling) bonds. Depending on the distance between two anion atoms with unsaturated bonds, the two anion atoms could interact (anion-anion wrong bond). The Te and Se atoms indicated by the black arrows have extra bonds. The dangling bonds, extra bonds, and wrong bonds are the main origin of the gap states created by GBs.

Because CdTe and CIS have similar structures and the atomic structures of the same type of GB are also very similar in these two compounds, one may expect similar electrical properties for GBs in CdTe and CIGS solar cells. However, electron-beam induced current image (EBIC) study has shown very different GB behaviors. Figures 4(a)

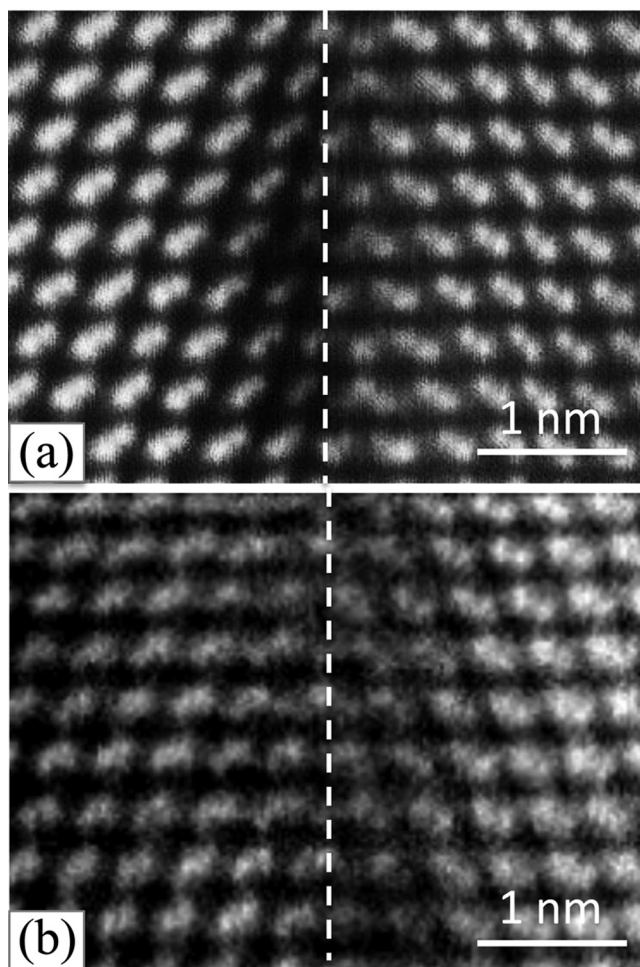


FIG. 2. Atomic-resolution aberration-corrected Z-contrast images of incoherent $\Sigma 3$ GBs in (a) CdTe and (b) CIGS.

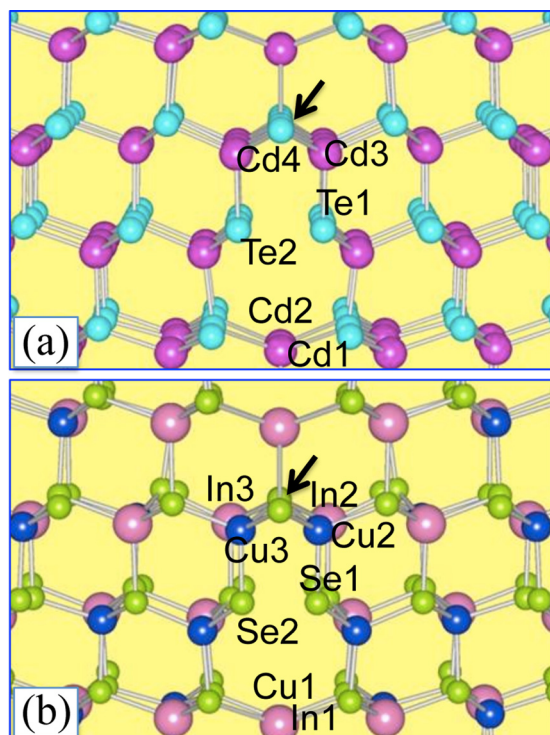


FIG. 3. Atomic structures of $\Sigma 3$ GBs in (a) CdTe and (b) CIGS.

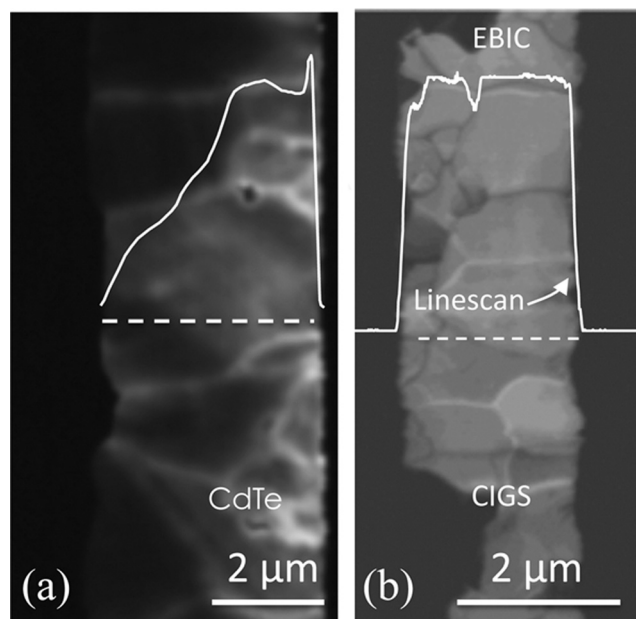


FIG. 4. Cross-sectional EBIC images obtained from devices with (a) CdCl₂ treated CdTe and (b) as-grown CIGS.

and 4(b) show cross-sectional EBIC images obtained from CdTe and CIGS thin-film solar cells, respectively. It is seen that GBs show much brighter contrast than the grain interiors in CdTe solar cells, whereas, only a small fraction of GBs show slightly brighter contrast in the CIGS sample. There are some GBs even showing darker contrast in the CIGS sample. The CdTe absorber went through a CdCl₂ heat treatment, but the CIGS absorber did not require any heat treatment. GBs in CdTe and CIGS clearly behave differently, which may be due to fundamental differences or different treatments such as the CdCl₂ heat treatment in CdTe and no treatment in CIGS solar cells.

To understand the difference, we first must understand how GB states are formed. Some general guidance on the formation of GB states can be drawn based on the atomic orbital theory. The formation of the conduction bands (CBs) and valence bands (VBs) of typical cation-anion compound semiconductors is depicted in Figure 5(a). The picture does not apply to CBs and VBs with partially occupied *d* orbitals and lone pair *s* orbitals. Typically, the CBs are derived from the *s*-orbitals of cation atoms, whereas the VBs are derived from the *p*-orbitals of the anion atoms. GBs with dangling bonds, extra bonds and wrong bonds will perturb the CBs and VBs and form GB states in the band gap. If the GB contains a cation atom with unsaturated bonds (dangling bonds), this atom will introduce donor like state(s) and it would lie between the CBM (the saturated case) and the cation atomic *s*-orbital level as indicated by D_d in Fig. 5(b). Likewise, the unsaturated anion atom will create acceptor state(s) lying between the VBM and the atomic anion *p*-orbital level as indicated by D_a in Fig. 5(b). However, if a GB contains cation-cation and anion-anion wrong bonds, the situation will be more complicated. As shown in Fig. 5(c), the cation-cation interaction may introduce bonding states (GS1) and anti-bonding states (GS1*). Similarly, the anion-anion

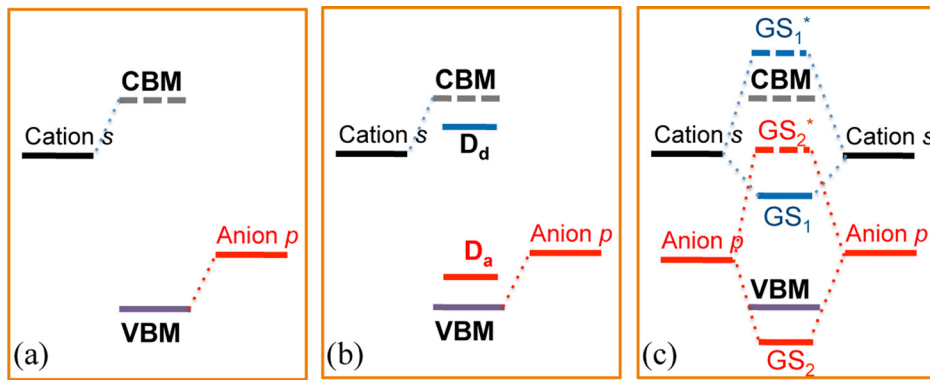


FIG. 5. Schematic showing the formation of GB states.

interaction will also introduce bonding states (GS_2) and anti-bonding states (GS_2^*). Depending on the relative energy positions between GS_1 and GS_2^* , electron transfer between these states may occur. The actual positions of these states depend on the lengths of the cation-cation and anion-anion bonds and can only be obtained via rigorous DFT calculations. Nonetheless, the picture indicates that for ionic semiconductors, the deep gap states are more likely formed by the wrong bonds.

Figure 6(a) shows the calculated band structure of the supercell containing a Te-rich GB in CdTe and the charge density map associated with the three gap states, GS_1 , GS_2 , and GS_3 , formed by the GB. It is seen that GS_1 and GS_2 states are created due to the Te-Te wrong bonding (marked Te1 and Te1 on Fig. 3). The GS_3 state is the bonding state of the Cd1-Cd2 wrong bonding. The calculated band structure and partial charge density maps of Se-terminated $\Sigma 3(114)$ GB in CIS are shown in Figure 6(b). It is seen that this GB also produce three gap states, GS_1 , GS_2 , and GS_3 . The formation mechanism of these gap states is very similar to the formation of the three gap states introduced by the $\Sigma 3(112)$ GB in CdTe. Here, the GS_1 and GS_2 gap states are derived from Se-Se (Se1, Se2) anion-anion wrong bonding and the GS_3 gap state is derived from Cu1-In1 cation-cation wrong bonding. Due to the size difference between Cu and In, the Se-Se wrong bonds have two different bond lengths, 2.50 Å and 3.28 Å. The shorter bond length results in a stronger Se-Se interaction. As a result, the antibonding state GS_1

from the shorter Se-Se coupling is pushed up close to the CBM, while the antibonding state GS_2 from the longer Se-Se coupling is deep in the gap. This explains why the separation between GS_1 and GS_2 states is larger in the $\Sigma 3(112)$ GB in CdTe than in the $\Sigma 3(114)$ GB in CIS.

The above analysis suggests that GBs in CdTe and CIGS should exhibit similar intrinsic properties. The observed difference in the EBIC images shown in Fig. 4 should not be fundamental, but rather be due to the different cell processes. Our recent studies have shown that in $CdCl_2$ heat treated CdTe thin films, Cl atoms segregate into GBs and substitute for Te atoms around GB cores in sufficiently high concentrations to invert them to n-type, creating local fields that enhance carrier collection as shown in Fig. 7.^{30,31} The results explain well why GBs in CdTe solar cells collect current more efficiently (brighter contrast in the EBIC image) than grain interiors after $CdCl_2$ heat treatment.

In CIGS solar cells, it has been found that:¹⁵ (1) GBs could be Cu-rich as compared to grain interiors. The Cu signals often anti-correlate with In signals, indicating that the excess Cu atoms are at In sites (Cu_{In}); (2) GBs contain high concentration of O. The O signals always anti-correlate with Se signals, indicating that O atoms occupy Se sites (O_{Se}); (3) The changes of composition at GBs are confined to regions of only about 1 nm, indicating the excess Cu and O atoms are located near GB planes. Our DFT calculations indicated that Cu_{In1} and O_{Se2} at the GB have much lower formation energies than other competitive defects in the whole range of

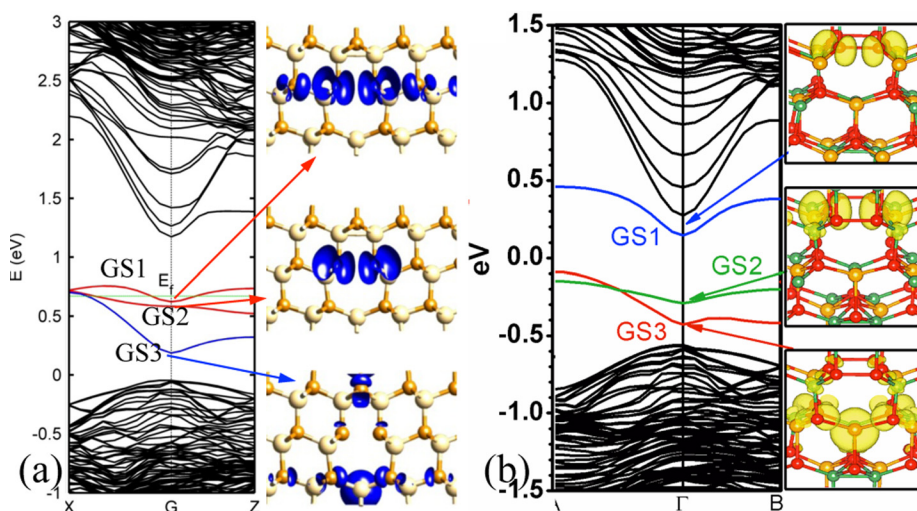


FIG. 6. The calculated band structures and partial charge density maps of $\Sigma 3$ GBs in (a) CdTe and (b) CIS.

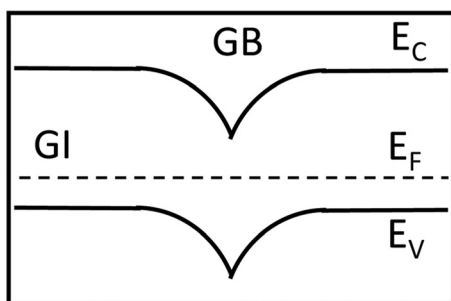


FIG. 7. A sketch showing the band diagram of the p-n-p junction at the GB.

chemical potential.²³ Our results therefore suggest that Cu_{In} and O_{Se} are the most stable defects and that they are confined at the boundary plane, which agrees well with the recent experimental results reported by Abou-Ras and co-workers.¹⁵ Figure 8(a) shows the atomic structure of a $\Sigma 3(114)$ GB in CIS with the segregation of $\text{Cu}_{\text{In}1}$ and $\text{O}_{\text{Se}2}$ at the GB. When a Cu atom substitutes for an In, the Cu-In wrong bond breaks. After full relaxation, the distance between Cu_{In} and Cu is 4.05 Å, which is significantly larger than the length of the Cu-In wrong bond (2.65 Å). Therefore, there is no coupling between $\text{Cu}_{\text{In}1}$ and Cu1, and the GS3 bonding state does no longer exist. Meanwhile, the GS1 moves closer to the CBM. When O_{Se} defects co-exist at the GB, the occupied GS2 deep gap state moves down into the VB of CIS, due to the stronger electronegativity and localization of O as compared to Se. Therefore, the segregation of Cu_{In} and O_{Se} can completely clean the gap states, as seen in the calculated band structure shown in Fig. 8(b), making the GB electrically benign. Our results suggest that GBs in CIGS are chemically modified so that they are not harmful to solar cell performance, especially the open circuit voltage. However, a benign GB may not enhance current collection as observed in CdTe. This may explain why many GBs in CIGS cells do not exhibit much brighter contrasts than grain interiors as seen in EBIC images.

IV. CONCLUSION

We have reviewed our atomistic theoretical understanding of the physics of GBs in CIGS and CdTe absorbers. We have shown that intrinsic GBs with dislocation cores

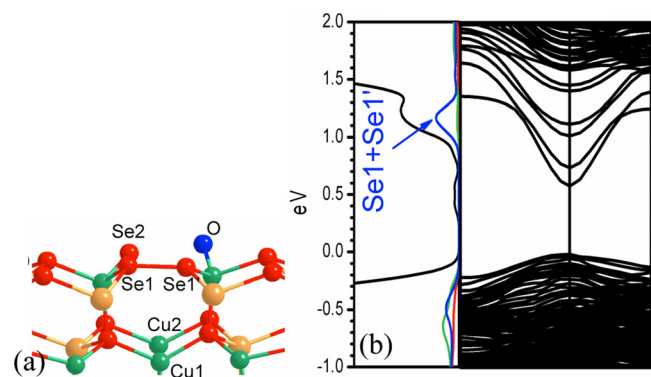


FIG. 8. (a) Atomic structure of a $\Sigma 3(114)$ GB in CIS with one Cu_{In} and one O_{Se} ; (b) calculated density of states and band structure of the GB with one Cu_{In} and one O_{Se} . Note the gap states have disappeared.

containing wrong bonds create deep gap states in both CIGS and CdTe and therefore are harmful to solar cell performance. However, the harmful effects may be suppressed through CdCl_2 heat treatment in CdTe or chemical modification in CIGS. In CdTe cells, Cl atoms segregating into GBs can convert the GB regions to n-type, forming local p-n-p junctions, which help current collections. In CIGS cells, GBs could be Cu-rich and contain O impurities. Such chemical changes can remove most of the gap states, making GBs benign. Our results suggest that the properties of GBs can be tuned through chemical modifications, providing guidance for future engineering of polycrystalline thin-film solar cells to achieve improved cell performance.

ACKNOWLEDGMENTS

This research used resources of the National Energy Research Scientific Computing Center, which was supported by the Office of Science of the U.S. Department of Energy under Contract No. DE-AC02-05CH11231. This work was supported by the U.S. Department of Energy (DOE) Office of Energy Efficiency and Renewable Energy, Foundational Program to Advance Cell Efficiency (F-PACE) and the national science foundation under Contract No. CHE-1230246. Work at NREL was supported by the U.S. Department of Energy under Contract No. DE-AC36-08GO28308. This work was also supported by ORNL's Center for Nanophase Materials Sciences (CNMS), which was sponsored by the Scientific User Facilities Division, Office of Basic Energy Sciences, U.S. Department of Energy. The authors thank R. Noufi, I. Repins, and S.-H. Wei for providing CIGS samples and stimulating discussions. Y.Y. acknowledges the support from the Ohio Research Scholar Program (ORSP).

¹See http://www.nrel.gov/ncpv/images/efficiency_chart.jpg for the record efficiencies of various solar cell technologies.

²J. Y. W. Seto, *J. Appl. Phys.* **46**, 5247 (1975).

³A. P. Sutton and R. W. Balluffi, *Interfaces in Crystalline Materials* (Oxford Science Publications, New York, 1995).

⁴H. J. Moller, *Semiconductors for Solar Cells* (Artech, Boston, MA, 1993).

⁵A. Rohatgi *et al.*, *Appl. Phys. Lett.* **84**, 145 (2004).

⁶X. Wu *et al.*, in *Proceedings of 17th European PVSEC*, 2001, p. 995.

⁷C. Persson and A. Zunger, *Phys. Rev. Lett.* **91**, 266401 (2003).

⁸C. Persson and A. Zunger, *Appl. Phys. Lett.* **87**, 211904 (2005).

⁹S. Siebentritt, S. Sadewasser, M. Wimmer, C. Leendertz, T. Eisenbarth, and M. C. Lux-Steiner, *Phys. Rev. Lett.* **97**, 146601 (2006).

¹⁰M. Hafmeiter, S. Siebentritt, J. Albert, M. C. Lux-Steiner, and S. Sadewasser, *Phys. Rev. Lett.* **104**, 196602 (2010).

¹¹D. Liao and A. Rockett, *J. Appl. Phys.* **91**, 1978 (2002).

¹²J. E. Jaffe and A. Zunger, *Phys. Rev. B* **64**, 241304 (2001).

¹³S. B. Zhang and S.-H. Wei, *Phys. Rev. B* **65**, 081402 (2002).

¹⁴Y. Yan, R. Noufi, and M. M. Al-Jassim, *Phys. Rev. Lett.* **96**, 205501 (2006).

¹⁵D. Abou-Ras, S. S. Schmidt, R. Caballero, T. Unold, H.-W. Schock, C. T. Koch, B. Schaffler, M. Schaffer, P.-P. Choi, and O. Cojocaru-Miredin, *Adv. Energy Mater.* **2**, 992 (2012).

¹⁶D. Cahen and R. Noufi, *Appl. Phys. Lett.* **54**, 558 (1989).

¹⁷L. Kronik, D. Cahen, and H. W. Schock, *Adv. Energy Mater.* **10**, 31 (1998).

¹⁸Y. Yan, C.-S. Jiang, R. Noufi, S.-H. Wei, H. R. Moutinho, and M. M. Al-Jassim, *Phys. Rev. Lett.* **99**, 235504 (2007).

¹⁹D. Abou-Ras, B. Schaffler, M. Schaffer, S. S. Schmidt, R. Caballero, and T. Unold, *Phys. Rev. Lett.* **108**, 075502 (2012).

- ²⁰S. S. Schmidt, D. Abou-Ras, S. Sadewasser, W. Yin, C. Feng, and Y. Yan, *Phys. Rev. Lett.* **109**, 095506 (2012).
- ²¹U. Rau, K. Taretto, and S. Siebentritt, *Appl. Phys. A* **96**, 221 (2009).
- ²²S. Siebentritt, M. Igalson, C. Person, and S. Lany, *Prog. Photovolt. Res. Appl.* **18**, 390 (2010).
- ²³W. J. Yin, Y. L. Wu, R. Noufi, M. M. Al-Jassim, and Y. Yan, *Appl. Phys. Lett.* **102**, 193905 (2013).
- ²⁴P. V. Meyers, C. H. Liu, and T. J. Frey, U.S. Paten No. 4,710, 589 (1 December 1987).
- ²⁵B. McCandless and R. Birkmire, *Sol. Cells* **31**, 527 (1991).
- ²⁶C. S. Ferekides, U. Balasubramanian, R. Mamazza, V. Viswanathan, H. Zhao, and D. L. Morel, *Sol. Energy* **77**, 823–830 (2004).
- ²⁷B. E. McCandless and K. D. Dobson, *Sol. Energy* **77**, 839–856 (2004).
- ²⁸I. Visoly-Fisher, S. R. Cohen, A. Ruzin, and D. Cahen, *Adv. Mater.* **16**, 879 (2004).
- ²⁹I. Visoly-Fisher, S. R. Cohen, K. Gartsman, A. Ruzin, and D. Cahen, *Adv. Funct. Mater.* **16**, 649 (2006).
- ³⁰C. Li, Y. Wu, J. Poplawsky, T. J. Pennycook, N. Paudel, W.-J. Yin, S. J. Haigh, M. P. Oxley, A. R. Lupini, M. Al-Jassim, S. J. Pennycook, and Y. Yan, *Phys. Rev. Lett.* **112**, 156103 (2014).
- ³¹J. Poplawsky, C. Li, N. R. Paudel, C. Li, C. Parish, D. Leonard, Y. Yan, and S. J. Pennycook, *Adv. Energy Mater.* **4**, 1400454 (2014).
- ³²W. K. Metzger and M. Gloeckler, *J. Appl. Phys.* **98**, 063701 (2005).
- ³³M. Gloeckler, J. R. Sites, and W. K. Metzger, *J. Appl. Phys.* **98**, 113704 (2005).
- ³⁴Y. Yan, M. M. Al-Jassim, and K. M. Jones, *J. Appl. Phys.* **96**, 320 (2004).
- ³⁵L. Zhang, J. Da Silva, J. Li, Y. Yan, T. Gessert, and S.-H. Wei, *Phys. Rev. Lett.* **101**, 155501 (2008).
- ³⁶G. Kresse and J. Furthmüller, *Phys. Rev. B* **54**, 11169 (1996); *Comput. Mater. Sci.* **6**, 15 (1996).
- ³⁷P. E. Blochl, *Phys. Rev. B* **50**, 17953 (1994).
- ³⁸G. Kresse and D. Joubert, *Phys. Rev. B* **59**, 1758 (1999).
- ³⁹J. P. Perdew and Y. Wang, *Phys. Rev. B* **45**, 13244 (1992).
- ⁴⁰S. L. Dudarev, G. A. Botton, S. Y. Savrasov, C. J. Humphreys, and A. P. Sutton, *Phys. Rev. B* **57**, 1505 (1998).
- ⁴¹H.-X. Deng, S.-S. Li, J. Li, and S.-H. Wei, *Phys. Rev. B* **85**, 195328 (2012).
- ⁴²W.-J. Yin, Y. Wu, S.-H. Wei, R. Noufi, M. M. Al-Jassim, and Y. Yan, *Adv. Energy Mater.* **4**, 1300712 (2014).
- ⁴³C. Li, Y. Wu, T. J. Pennycook, A. R. Lupini, D. N. Leonard, W. Yin, N. Paudel, M. Al-Jassim, Y. Yan, and S. J. Pennycook, *Phys. Rev. Lett.* **111**, 096403 (2013).
- ⁴⁴C. Li, J. Poplawsky, Y. Wu, A. R. Lupini, A. Mouti, D. N. Leonard, N. Paudel, K. Jones, W. Yin, M. Al-Jassim, Y. Yan, and S. J. Pennycook, *Ultramicroscopy* **134**, 113 (2013).